

STRUKTURA 2019

Žďár nad Sázavou, 10. 6. - 14. 6. 2019

Session I, Monday, June 10

L1

CRYSTALLOGRAPHIC SOFTWARE ON MALLEABLE HARDWARE

Z. Matěj¹, K. Skovhede^{1,2}, A. Barczyk¹, C. Johnsen², M. R. B. Kristensen², B. Vinter²

¹MAX IV Laboratory, Lund University, Sweden

²Niels Bohr Institute, University of Copenhagen, Denmark

zdenek.matej@maxiv.lu.se

X-ray laboratories have to deal with high data rates from novel high throughput cameras. Large scale facilities are developing plans for robust data reduction in order to moderate the data streams, simplify data storage, visualisation and analysis. For several applications traditional strategy of storing data first, and processing later presents a bottleneck and so real-time data reduction and analysis are receiving attention. Crystallographic software has been always keeping up with high performance computing. Effective implementation of crystallographic algorithms can be found even on graphical processing units [1-3]. However the range of “exotic” hardware for scientific computing is continually increasing, including digital annealers or the first commercial quantum computers already today. In this work so called field-programmable gate arrays (FPGAs) are used for non-trivial crystallographic data reduction. FPGAs present a sort of malleable computer hardware that is, already for decades, extensively used for readout of fast X-ray cameras or real-time applications controlling crystallographic experiments. However implementation of complex crystallographic analysis and data reduction codes on FPGAs is not common. The problem of azimuthal integration (AZINT) of streamed 2D-detector data for powder diffraction and small angle scattering is chosen here and implemented on FPGAs in order to demonstrate possibilities of this type of compute accelerators for more advanced data analysis in crystallography and other photon and neutron sciences. Future applications may include frame filtering, spot finding or diffraction features classification.

AZINT improves fundamentally the signal to noise ratio and allows detection of diffraction peaks even from noisy image data. The AZINT FPGA implementation allows for fixed and extremely short latencies in receiving integrated diffraction patterns that can be fitted in other parts of the configurable pipeline and provide a real-time feedback to the experiment. The solution can be integrated with compute infrastructures at large scale facilities or as an em-

bedded device it can increase capabilities of handling high throughput detector data in any lab. Azimuthal integration represents the first demonstration case of a project which aims for making FPGAs easily available for scientific software developers with use of industrial standards as OpenCL as well as with free and open-source numeric algebra toolbox based on synchronous message exchange (SME) [4].

This work was allowed beside others by advancements of FPGA platforms for data oriented computing and with evolution of appropriate programming models during the last decade. Compute FPGAs are excellent candidates for processing high throughput detector data. All the tasks of receiving, decompressing the camera image stream and the final AZINT computation can be handled on a single device. Initial benchmarks show that SME based implementation of a histogram computation, which is a basis of AZINT, can process 600 Gb/s [5] of uncompressed data stream.

1. G. Ashiotis, A. Deschildre, Z. Nawaz, J. P. Wright, D. Karkoulis, F. E. Picca, J. Kieffer, *J. Appl. Cryst.* **48**, (2015), 510-519. doi: [10.1107/S1600576715004306](https://doi.org/10.1107/S1600576715004306).
2. V. Favre-Nicolin, J. Coraux, M.-I. Richard, H. Renevier, *J. Appl. Cryst.* **44**, (2011), 635-640. doi: [10.1107/S0021889811009009](https://doi.org/10.1107/S0021889811009009).
3. I. Simecek, J. Rohlicek, T. Zahradnický, D. Langr, *J. Appl. Cryst.* **48**, (2015), 166-170. doi: [10.1107/S1600576714026466](https://doi.org/10.1107/S1600576714026466)
4. K. Skovhede, B. Vinter, in *FSP 2017; Fourth International Workshop on FPGAs for Software Programmers*, (2017), pp. 58-65.
5. C. Johnsen, *SME Binning*, github.com/bh107/SME-Binning (visited on May 6th, 2019).

eSSENCE@LU 5:10 project - Programmable hardware platform for scientific software - is kindly acknowledged for supporting this work..



L2

WHAT'S NEW IN THE POLYTIPIISM OF CRONSTEDTITE?

J. Hybler

*Institute of Physics, Academy of Sciences of the Czech Republic, Na Slovance 2,
CZ-182 21 Praha 8, Czech Republic
hybler@fzu.cz*

The layered silicate cronstedtite ($\text{Fe}^{2+}_{3-x}\text{Fe}^{3+}_x(\text{Si}_{2-x}\text{Fe}^{3+}_x)\text{O}_5(\text{OH})_4$, ($0.5 < x < 0.8$) provides relatively numerous polytypes generated by stacking 1:1 structure layers - OD packets with the trigonal protocell $a = 5.5$, $c = 7.1$ Å. Cronstedtite occurs rarely in low temperature hydrothermal deposits [1], in certain meteorites (CM chondrites) [2], and presumably on asteroids. Synthetic micrometer-size crystals were prepared by Pignatelli and her co-workers [1,3]. The data collected by four circle X-ray diffractometer with area detector processed by an appropriate software provide precession-like reciprocal space sections (RS sections) allowing for the determination of OD subfamilies (A, B, C, D), and particular polytypes. Similar RS sections are obtained by electron diffraction tomography (EDT), for small crystals [1].

The synthetic material contains mainly $1M$ and $2M_1$ polytypes (subfamily A), sometimes twinned by the 120° rotation around c_{hex} axis. The $3T$ polytype (subfamily A) is less common. Only one rare mixed crystal of the $1M$ and $1T$ polytypes of A and C subfamilies, respectively was identified, too. Another, apparently ninetuple polytype with metrically R -centred lattice is in fact triclinic, because of the lack of a threefold axis. It is thus denoted as $3A$. Common diagrams for determination of polytypes were generalized in order to include non-trigonal and non-hexagonal polytypes [1].

Several new occurrences were studied. Cronstedtite crystals from Nagybörzsöny, Hungary, contain nice examples of the well-ordered $1M$ polytype, pure or in mixed crystals with $3T$. In some crystals, the $1M$, in another the $3T$ polytype is dominant. The twinning by the 120° rotation around c_{hex} axis is also present in some crystals. Moreover, totally or almost disordered crystals with diffuse streaks instead of characteristic reflections were found.

Very promising appeared the new occurrence Ouedi Beht, El Hammam, Morocco, about 80 km SEE from Rabat (GPS $33^\circ 33' 15.19''\text{N}$, $5^\circ 49' 53.68''\text{W}$). The locality is represented by a small pit in the mountains. Of the A subfamily: polytypes $3T$, $1M$, $2M_1$, $6T_2$ (previously described from Pohled, ČR) [4,5] were identified. Monoclinic polytypes occur not separately, but always in

mixed crystals, like $1M+3T$, $2M_1+3T$, $1M+2M_1$, $2M_1+6T_2$. Again, monoclinic polytypes are often twinned by the 120° rotation around c_{hex} axis. $2H_1$, $2H_2$ polytypes of the subfamily D are also common. Moreover, a sextuple polytype was identified in one separate crystal and in many mixed crystals with $2H_1$. It is not yet clear, whether it is identical with the $6T_1$, described by Hall et al [6]. The polytype $6R$ was found as dominant in one mixed crystal with $2H_1$. Another sextuple R -centred polytype was found in one rare crystal, twinned by 60° rotation around c_{hex} axis (the so-called obverse-reverse twin).

It is worth noting, that the participants of the colloquium, who used a train from Prague to Žďár nad Sázavou, passed closely near two localities of cronstedtite: Rejské Lode at Kaňk (the hill right from the line, just before approaching the station Kutná Hora), and Pohled (the quarry at the right side, after passing the station Pohled). Other two localities Chvaletice (indicated by a chimney of the power station) and Litošice (approximately in the same direction, hidden in the forest) are somewhat distant from the line.

Author thanks Martin Števkó for providing samples from Nagybörzsöny and Morocco.

- Hybler, J., Klementová, M., Jarošová, M., Pignatelli, I., Mosser-Ruck, R., Ďurovič, S. *Clays and Clay Minerals*, **66**, (2018), 379–402. DOI: 10.1346/CCMN.2018.064106.
- Pignatelli, I., Mugnaioli, E., and Marrocchi, Y. *European Journal of Mineralogy* (2018), DOI: 10.1127/ejm/2018/0030-2713.
- I. Pignatelli, E. Mugnaioli, J. Hybler, R. Mosser-Ruck, M. Cathelineau, N. Michau, *Clay. Clay Miner.*, **61**, (2013), 277.
- J. Hybler, J. Sejkora, V. Venclík, *Eur. J. Mineral.*, (2016), DOI: 10.1127/ejm/2016/0028-2532.
- J. Hybler, *Eur. J. Mineral.*, (2016), DOI: 10.1127/ejm/2016/0028-2541.
- Hall, S. H., Guggenheim, S., Moore, P., Bailey, S. W. *Can. Mineral.* **14**, (1976), 314-321.

APPLICATION OF POWDER X-RAY DIFFRACTION FOR HEAVY MINERAL PROSPECTION IN THE CZECH REPUBLIC

M. Čurda, F. Laufek, T. Sidorinová, M. Štrba

Czech Geological Survey, Geologická 6, 152 00 Praha
michal.curda@geology.cz

The government of the Czech Republic has adopted a resolution no. 717 concerning the economic interests of the Czech Republic in the area of super strategic minerals resources and other minerals resources. Consequently, the state company DIAMO and the Czech Geological Survey were charged with a task to perform the evaluation and an update of strategic minerals resources of the Czech Republic [1, 2].

A regional prospection for heavy minerals (i.e. minerals with density higher than 2.9 g/cm^3) is an integral part of this project. This activity involves collection of selected samples in the field, mineral separation and subsequent quantitative phase identification. Traditionally, *optical identification* of separated mineral grains using binocular microscopes has been the most used method for such task. However, this method has several disadvantages, e.g. difficulties in identification of some mineral phases, high-time demands and others. Moreover, only well-qualified and experienced analyst can produce reliable results.

Another way of quantitative phase analysis of heavy minerals is an application of so-called *automated mineralogy methods*. Automated mineralogy analytical solutions are characterised by integrating largely automated measurement techniques based on Scanning Electron Microscopy (SEM) and Energy-dispersive X-ray spectroscopy (EDS). In addition to the quantitative phase analysis, this method can provide information concerning the size and shape of analysed grains, relations between minerals (e.g. their intergrowths) [3]. Nevertheless, there are several disadvantages including e.g. the difficulty to distinguish between mineral polymorphs (e.g. TiO_2 or Al_2SiO_5 polymorphs) or complex preparation of studied samples. The price of such analysis is also relatively high, which complicates its routine application.

Powder X-ray diffraction (PXRD) with subsequent Rietveld data analysis seems to be an effective alternative method for such task. Preliminary analyses were performed at Laboratory of X-ray Diffraction of the Czech Geological Survey at Bruker D8 Advance diffractometer. The CuK radiation, positive-sensitive detector Lynx Eye XE and 9-position sample changer (Flipstick) for reflection were used for measurement. Application of fast positive-sensitive detector and sample changer enabled fast data collection and high output from the Laboratory including automated nights measurements. Using the above-mentioned instrumentation, it is possible to measure 18 samples per day. Contrary to the methods of automated mineralogy, it is possible to distinguish between different polymorphs and the preparation of samples is relatively easy. On the other hand, a careful mineral separation of heavy minerals sample into several concentrates is necessary. Prior to diffraction analyses, the heavy minerals samples are separated according to their specific gravity and magnetic properties. The resulted fractions are weighted and subsequently analysed by PXRD. Qualitative analysis is performed in the HighScore program, subsequent quantitative analysis is carried out by the Rietveld method. A program Topas 5 is used.

In this contribution, first experiences and preliminary results of quantitative phase analysis of heavy minerals concentrates by PXRD will be discussed. It seems that PXRD might be an interesting method for such a mineralogical analysis.

1. P. Rychtařík, *Podnikový občasník s.p. DIAMO*, **11**, (2017).
2. M. Žáček, M. Francírek, L. Hůlka, *GEOMIN s.r.o.*, (2018).
3. T. Hrstka, P. Gottlieb, R. Skála, K. Breiter, D. Motl, *Journal of Geosciences*, **63**, (2018), 47-63.

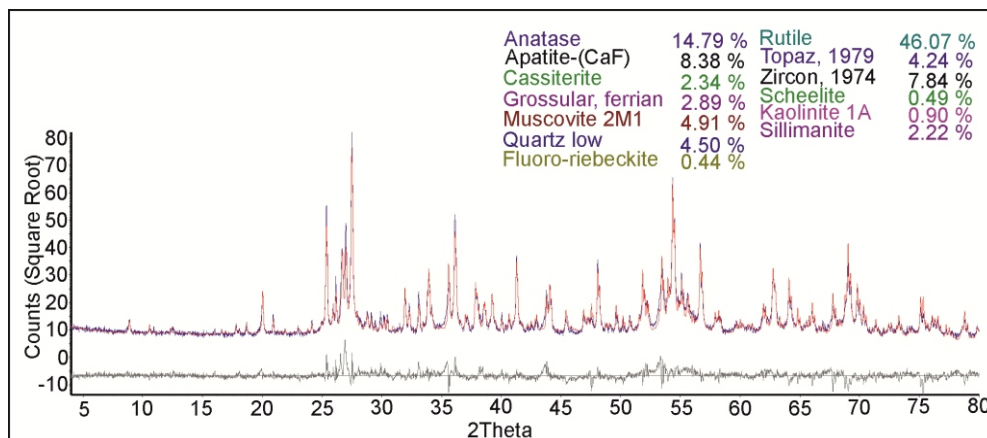


Figure 1. Typical Rietveld plot of the heavy mineral concentrate showing wt.% of minerals.



L4

CRENEL OR NOT CRENEL, WHAT IS THE FUNCTION?

Elen Duverger-Nédellec¹, Kateryna Bretosh², Virginie Béreau², Carine Duhayon²,
Jean-Pascal Sutter², Václav Petříček³

¹Charles University, Faculty of Mathematics and Physics, Condensed Matter Department, Ke Karlovu 3,
121 16 Praha 2, Czech Republic

²Laboratoire de Chimie de Coordination du CNRS, Université de Toulouse, 31077 Toulouse, France

³Institute of Physics CAS, Department of Structure Analysis, Na Slovance 1999/2, 182 21 Prague 8,
Czech Republic

Modulated structures are not a piece of cake to solve but some of them can be trickier than the others. The most obvious solution is not always the proper one and conscientious verifications of the model have to be done in order to obtain the best structural model. We will focus here on the example of the (3+1)D structure of the FeLN5PhenMeCl2 complex presenting a typical misleading modulation.

The resolution and refinement of the structure were performed using the software Jana2006 [1]. The average structure of FeLN5PhenMeCl2 was determined using Superflip program [2]. The structure is composed of two superimposed inversed configurations of the complex, indicating the presence of disorder. This disorder is the tricky point of the structural resolution! To model it, two options can be considered: the use of a crenel-type occupational modulation [3] or the use of a sinusoidal occupation-function coupled with a positional modulation function. In the first case, the disorder observed in the average structure is,

in fact, a hidden-order: both configurations would exist independently, appearing alternately along the periodicity axis of the modulation. In the second case, the disorder can reflect an ordered-disorder along the fourth dimension: each configuration presents a positional modulation (the order) and a probability of presence given by the occupational modulation (the disorder). Both possibilities will be investigated. Final structures will be observed via the new graphic tool developed in Jana2020 [4] enabling the direct observation of mixed modulations on the structure.

1. V. Petříček, M. Dušek, L. Palatinus (2014), *Z. Kristallogr.* 229(5), 345-352.
2. L. Palatinus, G. Chapuis (2007), *J. Appl. Cryst.*, 40, 786-790.
3. V. Petříček, A. van der Lee, M. Evain (1995), *Acta Cryst.* A51, 529-535.
4. V. Petříček, M. Dušek, L. Palatinus (2020) to be published.

L5

STRUCTURAL ANALYSIS OF NANOPOROUS GOLD OBTAIN BY DEALLOYING

Adrien Chauvin¹, Lukas Horak¹, Elen Duverger-Nédellec¹, Milan Dopita¹, Pierre-Yves Tessier², and Abdel-Aziz El Mel²

¹Charles University in Prague, Ke Karlovu 3, 121 16 Praha 2, Czech Republic

²Institut des Matériaux Jean Rouxel, Université de Nantes, CNRS, 2 rue de la Houssinière B.P. 32229,
44322 Nantes cedex 3, France

adrien.chauvin@karlov.mff.cuni.cz

Nanoporous materials are of great interest since a few decades due to their high specific surface area and their three-dimensional porosity. These materials, constituted of interconnected ligament structure, can be used in a wide range of areas such as biotechnology [1], electronics [2] or energy storage [3]. The most used technique for the creation of a nanoporous structure is the dealloying process. Briefly, it consists in the dissolution of the less noble metal from an alloy resulting in the formation of a three-dimensional skeleton of the more noble element at nanoscale. Nowadays, lots of work has been devoted to tune the final nanoporous structures, i.e. ligament sizes and porosity, and improve their properties. These techniques include, for example, the modification of the dealloying kinetic or by further annealing the nanoporous structure. However, only a few studies report on the modification of the morphology of as-grown alloy. Indeed, controlling the morphology and

the residual stress in thin films after the growth of materials is crucial to tailor their properties. Although the presence of residual stress in a thin film is in general considered as a drawback, however in some particular cases, it can be of real benefit for the desired application. In this contribution, I will show how the residual stress in a deposited gold copper alloy by magnetron co-sputtering can be used to tune the morphology of nanoporous gold after dealloying. Deposition of a gold copper thin film was performed over a substrate at different temperature leading to different morphologies of the thin film according to Thornton diagram. Dealloying those thin films in nitric acid lead to an island-like nanoporous morphology for high deposition temperature. The origin of such innovative morphology is attributed to the remaining stress in the sample after deposition (Figure 1). More precisely, it has been demonstrated that the residual stress is mostly due to the thermal stress in-

duced during deposition. In this study, the remaining stress in as-grown films was studied by X-ray diffraction analysis and the nanoporous structure was probed by Small Angle X-ray Scattering and Scanning Electronic Microscopy. Such nanostructured gold thin film with a double level of porosity can be considered as potential candidates for the development of advanced sensors and actuators.

1. W. Gao and J. Wang, *Nanoscale*, **6**, (2014), 10486.
2. A. Chauvin, W. Txia Cha Heu, J. Buh, P.-Y. Tessier and A.-A. El Mel, *NPJ Flexible Electronics*, **3**, (2019).
3. X. Lang, A. Hirata, T. Fujita and M. Chen, *Nature Nanotechnology*, **6**, (2011), 232.

The authors acknowledge the financial support from the project NanoCent—Nanomaterials Centre for Advanced Applications, Project No. CZ.02.1.01/0.0/0.0/15_003/0000485, financed by ERDF.

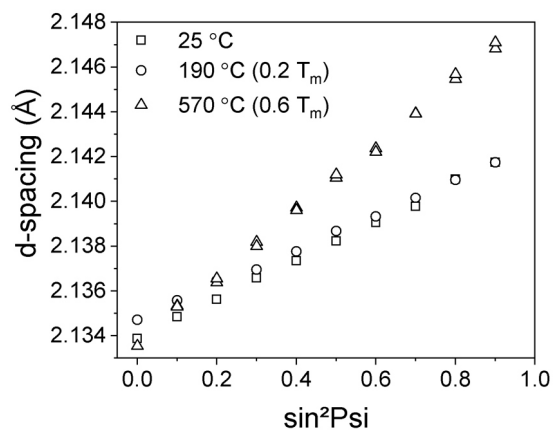


Figure 1. Evolution of the d-spacing as a function of \sin^2 in as-grown thin film at different temperatures.